*Journal of Ceramic Processing Research. Vol. 26, No. 4, pp. 680~689 (2025)*
*(Received 29 May 2025, Received in revised form 20 July 2025, Accepted 24 July 2025)*
*https://doi.org/10.36410/jcpr.2025.26.4.680*

J O U R N A L O F
**Ceramic Processing Research**

# Synthesis, characterization, and machinability of copper matrix composites reinforced with micro and nano-sized $Si_3N_4$ and AlN particles

**Harikishore S[a,*] and Mathalai Sundaram C[b]**
[a]*Assistant Professor and Corresponding Author, Department of Mechanical Engineering, Nadar Saraswathi College of Engineering and Technology, Theni - 625531, Theni District, Tamil Nadu, India*
[b]*Professor, Department of Mechanical Engineering, Nadar Saraswathi College of Engineering and Technology, Theni - 625531, Theni District, Tamil Nadu, India*

**The present study investigates the synthesis, characterization, and machinability evaluation of copper matrix composites reinforced with silicon nitride ($Si_3N_4$) and aluminum nitride (AlN) particles in both micro and nano forms. Composites containing 5 wt.% of each reinforcement were fabricated using a powder metallurgy route involving ball milling, cold compaction, and sintering at 800 °C. The resulting composites were characterized for density, porosity, and microhardness in accordance with ASTM standards. SEM and EDS analyses confirmed uniform distribution and high purity of the reinforcements without evidence of interfacial reaction products. Among all compositions, the $Si_3N_4$ micro-particle reinforced composite exhibited the highest hardness (68 HV) and density (6.24 g/cc), indicating superior particle-matrix bonding. In contrast, AlN-reinforced samples exhibited better dispersion and ductility but lower mechanical strength, with densities around 5.57 g/cc. Machinability was assessed using wire electrical discharge machining (WEDM), where $Si_3N_4$ based composites demonstrated finer surface finishes (minimum Ra ~2.5 µm), while AlN reinforced composites with micro particles exhibited rougher surfaces and higher oxide formation. These findings highlighted the effectiveness of $Si_3N_4$ micro-particle reinforcement in enhancing the mechanical and machining performance, making it suitable for copper composites to be utilized in frictional and structural applications.**

**Keywords: Copper matrix composites, Silicon nitride, Aluminum nitride, Micro/nano reinforcement, Powder metallurgy, WEDM, Surface roughness.**

## Introduction

Copper-based composite materials are widely utilized across various engineering domains due to their excellent thermal conductivity, electrical conductivity, and desirable mechanical and electrochemical properties [1]. These characteristics make copper matrix composites (CMCs) ideal candidates for structural and mechanical load-bearing systems. Typically, these composites are developed by reinforcing soft copper matrices with hard ceramic particles through manufacturing methods such as powder metallurgy, stir casting, mechanical alloying, and friction stir processing [1, 2].

In recent years, materials intended for frictional and wear-resistant applications have seen increased demand, particularly those produced using powder metallurgy routes for better structural integrity and homogeneity. Studies have stated that reinforced copper-based composites with hard ceramic or fiber reinforcements are ideal for such applications [3]. Reinforcements like alumina ($Al_2O_3$), silicon carbide (SiC), tungsten carbide (WC), zirconia ($ZrO_2$), chromium (Cr), and carbon nanostructures such as graphene or CNTs have been explored extensively for their wear-resistant properties [4]. Composite systems such as Cu–Cr–SiC [5] and CuNiSiCr alloys [6] have shown promising results for thermal and mechanical reliability. Additionally, composites reinforced with $Zr_2Al_3C_4$ are under investigation for structural and electrical applications [7].

Recent studies have further highlighted the potential of ceramic reinforcements in metal matrix composites. FStudies have developed a laminated $Si_3N_4$/BN-$Al_2O_3$ structure that exhibited high fracture toughness and flexural strength, showcasing the benefit of tailored ceramic microstructures for mechanical performance improvement [8]. Machinable $B_4C$/BN composites were investigated, and it was found that nanocomposites performed significantly better than microcomposites in terms of fracture strength, thermal shock resistance, and surface finish, thereby emphasizing the advantages of nanoscale reinforcements [9].

Moreover, the role of $Si_3N_4$ and $TiO_2$ nanoparticles in functionally graded Al7075 composites was explored, and enhanced hardness, tensile strength, and wear resistance

*Corresponding author:
Tel : +91 9677406940
E-mail: harikishoreidea@gmail.com

due to the graded distribution of reinforcements were demonstrated [10]. This is further supported by the report that the addition of SiC, $TiO_2$, and Ni–Gr nanoparticles significantly improved both mechanical and electrical discharge machining performance in LM26 aluminium matrix composites [11].

For AlN-based systems, recent advancements have focused on synthesis and processing optimization. An improved carbothermal reduction–nitridation method for AlN synthesis was proposed, and superior purity and thermal conductivity were achieved through controlled decarbonization and high-temperature treatment [12]. It was also demonstrated that AlN nanopowders with uniform particle size (30–90 nm) could be synthesized using microwave-assisted combustion methods, making them ideal for nano-reinforced composites [13].

Despite the significant progress in ceramic-reinforced copper and aluminum-based composites, the development of Cu matrix composites reinforced with silicon nitride ($Si_3N_4$) and aluminum nitride (AlN) remains underexplored. Particularly, studies comparing the effects of micro vs. nano-sized ceramic reinforcements on the mechanical and machining performance of Cu composites are sparse. Additionally, conventional machining techniques pose challenges due to the high hardness of the composite surface, making wire electrical discharge machining (WEDM) a more viable alternative for precise and effective material removal [14]. Milling and edge cutting operations are difficult to machine the copper and copper base composites [14, 15]. In order to improve the machinability of copper base composite material, unconventional machining process could be chosen.

From the above literatures, it is clear that while many ceramic reinforcements have been extensively explored in aluminum and hybrid metal matrices, research on $Si_3N_4$ and AlN in copper-based composites, especially with attention to particle scale (micro vs. nano), densification, and machinability, is limited. This study aims to fill this research gap by fabricating Cu-based composites reinforced with both micro- and nano-sized $Si_3N_4$ and AlN particles via powder metallurgy, followed by a comprehensive evaluation of their microstructural integrity, mechanical properties, and WEDM machinability.

## Materials and Methods

### Materials

A 99.99% pure copper powder is used as a matrix material to develop the composite with two different reinforcements. The two different reinforcements such as silicon nitride ($Si_3N_4$) and aluminum nitride (AlN) were used as a reinforcement material to develop Cu – $Si_3N_4$ and Cu – AlN based composite material. The size of the copper material is 30 μm and the reinforcement were varied with two different (micro level and nano level) sizes such as Cu – $Si_3N_4$ NP (nano level), Cu – $Si_3N_4$ μP (micro level), Cu – AlNNP and Cu – AlNμP. The weight percentage of the reinforcement is maintained as 5 wt.% [16, 17] for all the four combinations.

### Methods

To promote uniform blending with the copper powder and avoid particle agglomeration, a ball milling machine was used to blend the reinforcement and the base metal matrix powders using a planetary ball mill which has been spun at a speed of 250 rpm continuous for 60 minutes [18]. This procedure ensured adequate dispersion of both nano- and micro-sized particles within the Cu matrix without inducing excessive cold welding or work hardening [19]. Subsequently, powder compaction was done with a stainless-steel mold for a diameter of 12 mm for all the samples. In order to improve green compaction, the length of the rod is maintained as 120 mm, following an aspect ratio of 1:10. Following green compaction, all of the samples are sintered (heat treated) in a box furnace for three hours at a constant temperature of 800 °C [20].

After the post-sintering treatment of the green compacted samples, all specimens were tested and evaluated in accordance with relevant ASTM standards. Density measurements were conducted following ASTM D792-20, microhardness testing was performed as per ASTM E92-2023, and porosity was determined using standard procedures. Each sample was metallographically polished using progressively finer grit papers, followed by alumina polishing to reveal the microstructure of the sintered Cu-based composites. -Microhardness testing was carried out according to ASTM E92-2023. For each composite sample, five indentations were made at different regions (uniformly spaced) on the polished cross-section, and the average value was reported. The standard deviation was calculated and remained within ±2 HV for all test groups, indicating high consistency. For machinability analysis, the wire electrical discharge machining (WEDM) process was employed using a CNC wire-cutting machine (Model: Electronica BMG 830) equipped with a 0.25 mm Cu-Zn half-hard wire. The process parameters used during slicing are listed in Table 1.

To ensure repeatability, three specimens were machined per composite composition under identical WEDM conditions. Surface roughness (Ra) measurements were taken at three different positions along the cut surface for each specimen using a calibrated (Model: Mitutoyo SJ210) surface roughness tester (ISO 4287). The averaged values were used for analysis, and the variation between replicates was minimal (standard deviation <0.2 μm in all cases). The machined surfaces were further examined under a scanning electron microscope to assess surface topography and validate machining consistency.

**Table 1.** The process parameter of wire electrical discharge machining to slice the Cu base composite material.

| Parameters | Range | Units |
|---|---|---|
| Voltage | 50 | Volt |
| Cutting speed | 1 | mm/min |
| Duty factor | 90 | % |
| Wire tension | 7 | kg/mm |
| Pulse off time | 10 and 30 | µs |
| Pulse on time | 110, 115 and 120 | µs |
| Electrolyte | Deionised water | |

## Results and Discussion

### Material Synthesis and Composite Development

A particles analyzer which is used to measure the particles of Cu powder and the reinforcement powders are measured and the values are provided in the Table 2. Fig. 1 shows the scanning electron image of pure copper powder used for composite development. The copper particle is 99.99% in purity and particle size are in the range of 31 µm, revealed to be in a spheroidal shape. The copper powders are face center cubic in crystal structure and they are spheroidal in shape. The spheroid shape of the copper possesses high malleability and they are recommended for powder compaction composite development.

**Table 2.** Particle analyzer for base metal powder and reinforcement particles.

| Sample No. | Powder particle | Mean (µm) | Standard deviation |
|---|---|---|---|
| 1 | Cu | 31.119 | 0.439 |
| 2 | $Si_3N_4$ NP | 0.486 | 0.639 |
| 3 | $Si_3N_4$ µP | 20.80 | 0.644 |
| 4 | AlNNP | 0.634 | 0.416 |
| 5 | AlNµP | 50.25 | 0.363 |

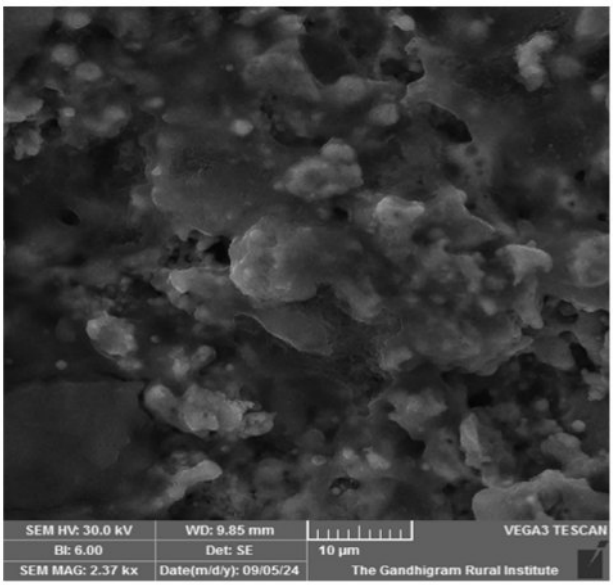


**Fig. 1.** Cu SEM Image.

The structural morphology of the reinforcements $Si_3N_4$ NP, $Si_3N_4$ µP, AlNNP and AlNµP are observed through the electron microscopy and presented in the Fig. 2. The powder morphology of the reinforcements is irregular in shape and the particle sizes are invariant. Maximum size of the $Si_3N_4$ NP is measured as around 0.486 µm (around 75% in particle size distribution) and the remaining weight percentage has a maximum particle of size 1.84 µm; to a standard deviation of 0.644. Similarly, the AlNNP with a minimum size of 0.634 µm and maximum of 3.46 µm (for 25 wt.%). The $Si_3N_4$µP

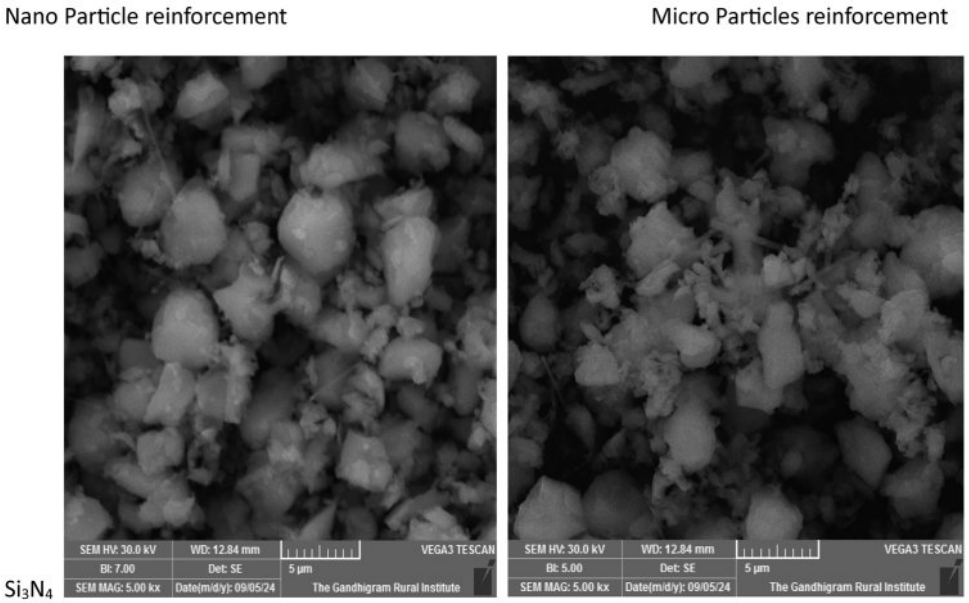

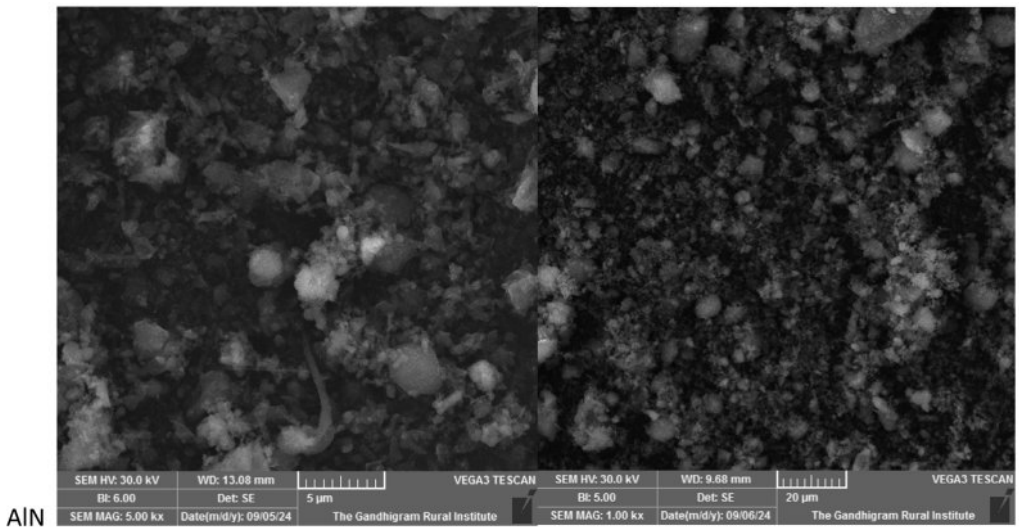


**Fig. 2.** Electron image of the reinforcement particle for comparison.

and AlNµP particles are measured to a maximum 20.80 µm and 50.25 µm in particle size. The collection of nano particles is very fine and it is individual (discrete) in nature compared to the micro size particles. The quality of the particle is further verified using Energy Dispersive Spectroscope (EDS) to read the elements of the nano/micro reinforcement particles. Fig. 3 indicates the backscattered image (BSE image) and spectra data of the $Si_3N_4$NP, $Si_3N_4$µP, AlNNP and AlNµP reinforcement powders. The quality of the reinforcement particle is verified and it is evident that, the purity of powder is about 99% and the same has been used for Cu based composite development. Additionally, the conventional compaction method is used to create the copper base composite with reinforcement. Two distinct reinforcing combinations ($Si_3N_4$ and AlN) are used to make the Cu base composite, and two factors (nano and micron) in particle size are proposed as indicated in Table 3. The process of green compaction and sintering were performed following the standard procedure as given in the previous section. The Cu developed through the powder compaction are heat sintered under inert atmosphere and they are evaluated to report the metallurgical quality in terms of micro structure and phase distribution.

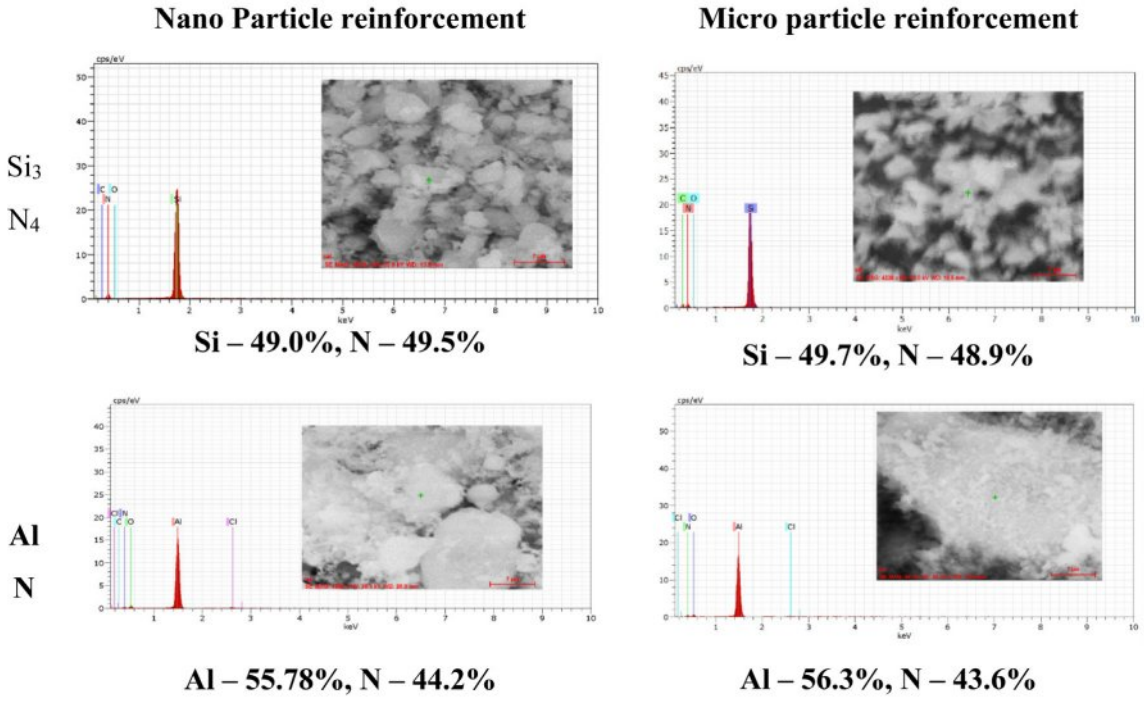


**Fig. 3.** BSE Image and EDS analysis of reinforcement particle.

**Table 3.** Proportion of Cu based composites.

| Sample no | Base metal | Reinforcement | Total wt. of the powder |
|---|---|---|---|
| 1 | Cu – 100% | - | 35g |
| 2 | Cu – 95% | $Si_3N_4$NP – 5% | 32g |
| 3 | Cu – 95% | $Si_3N_4$µP – 5% | 32g |
| 4 | Cu – 95% | AlNNP – 5% | 31.5g |
| 5 | Cu – 95% | AlNµP – 5% | 31.5g |

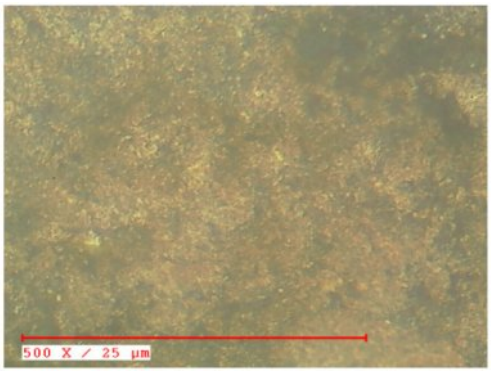


**Fig. 4.** Pure Cu particle after compaction and sintering.

## Metallurgical and Mechanical Properties of Cu base composite

The micro structure of the copper powder after compaction and sintering are metallurgically polished to reveal the microstructure using the potassium dichromate as an etchant. Microstructure of the pure copper rod is sliced and observed in the middle section (cross section) of the rod. Fig. 4 shows the optical image of the pure Cu rod developed through powder compaction. Microstructure of the Cu rod reveals with a cluster of grains as an irregular polygon and fibrous in the shape. This structural formation is due to the deformation (compression force) of spherical metal powder during compaction. The grain boundaries are irregular in size with good metallurgical bonding [19, 21]. Sintering the green compaction at 700 °C for a maximum soaking duration of three hours strengthens the binding between the grains. Subsequently, the Cu base composite with different reinforcement materials is also observed through the optical microscope after polishing and etching the samples.

Fig. 5 shows the optical images of Cu composite with different reinforcement particles. The Cu base matrix

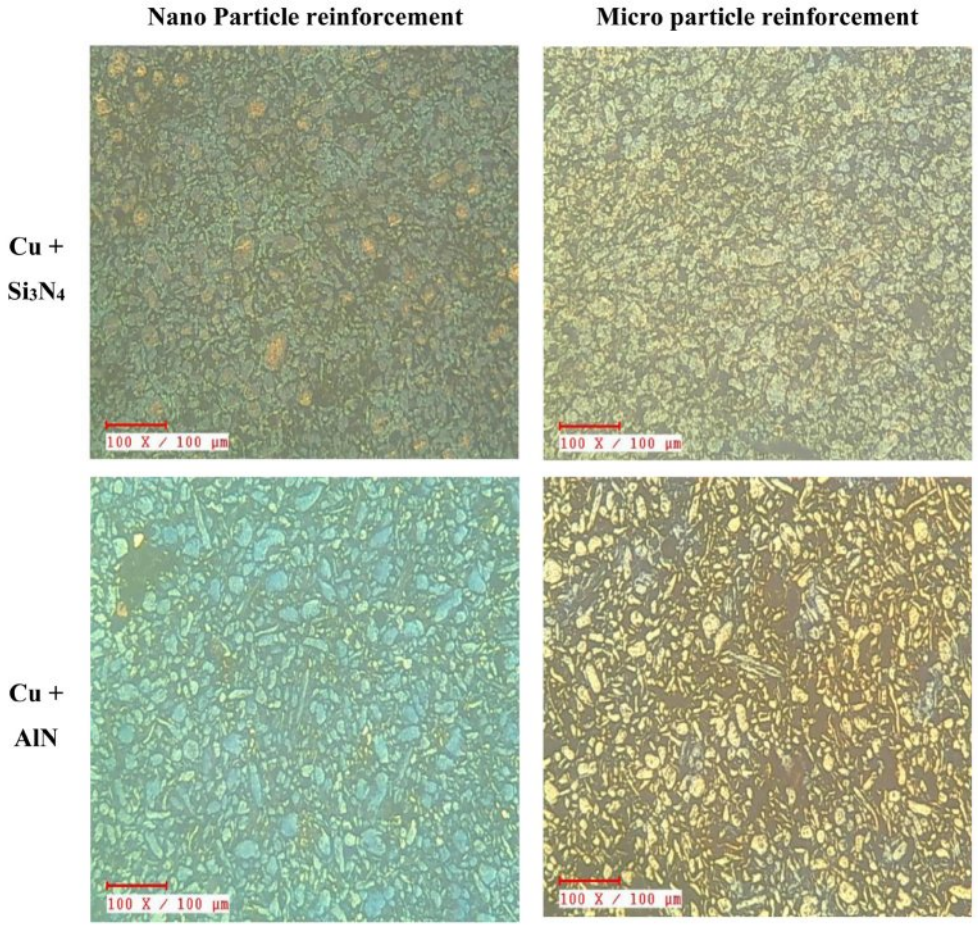


**Fig. 5.** Optical image of Cu – $Si_3N_4$ and Cu – AlN reinforced composite.

material is a continuous phase reveal (dark colour) and the reinforcements (with light colour) are uniformly distributed throughout the cross-sectional area of the base metal. The spherical copper particle has undergone severe deformation during the powder compaction and grain boundaries were revealed with a strong bonding due to sintering temperature for a standard time. Literatures with similar reinforcements are observed with similar morphological structures [3, 21]. Let us infer the Cu metal powder with $Si_3N_4$ reinforcement particle with different particle size. Basically, the $Si_3N_4$ powder possess low contact angle indicating the minimum wettability for the powder compaction [22]. During compaction, the reinforcement of $Si_3N_4$ powder in the Cu matrix found to be equally distributed and metallurgical bonding as depicted in Fig. 5. The distribution of nano level $Si_3N_4$ powder in the Cu matrix has dense structural results compared to the micro level $Si_3N_4$ powder. This may be due to the impregnation of nano size particle through the coarse Cu particle during compaction. Similarly, the rate of agglomeration (matrix material) is more and uneven in micro level $Si_3N_4$ powder while compared to the nano level particle reinforcement. For the Cu + AlN composite the white layer (Cu phase) dispersion rate was found to be very less as the wettability of AlN helped to get fused with the Cu particle easily [23, 24]. In general, the AlN are super ductile and highly deformable to mix up with Cu matrix material. Further the Cu base composites are evaluated for micro hardness, density and porosity following the ASTM standards.

Using the ASTM standard procedure, the basic properties of the copper base composite for density (ASTM D 792 – 20) and micro hardness measurement (ASTM E92 – 2023) were evaluated. The micro hardness of the pure copper rod is 50±2 Hv as per the literature report. From the experimentation the pure copper rod made through the powder compaction method has reported to be in the range of 49 Hv as given in the Table 4. Similarly, the $Si_3N_4$ reinforced Cu base composite material has found to be at an average of 68 Hv with $Si_3N_4$μP and 59 Hv for the $Si_3N_4$NP reinforced Cu base composite material. Subsequently, the AlN reinforced copper base composite materials have 54 Hv for nano particles and 65 Hv for micro particle reinforcement. The presence of $Si_3N_4$ particle in the copper matrix was found to be increased with nano level particle compared to the micro level particle. The hardness of $Si_3N_4$ particle has increased to a maximum of 18% and a 38% increase for AlN particle over the pure copper matrix material. The results on density and porosity are evaluated for factorial combination with comparative analysis. Pure Cu matrix material was measured to a maximum of 6.1 g/cc and the reinforcement of $Si_3N_4$ particle in the Cu matrix is 6.24 g/cc compared to the base metal which is 6.1 g/cc. However, the density of the AlN reinforced Cu base composite is considerably lesser (5.57 to 5.7 g/cc) than the $Si_3N_4$ particle in the Cu composite and the matrix material. The porosity of the Cu base composite material is in the range of 1.9 to 3.1 percentage which is found to be a considerable rate for a good composite as referred from the literatures. This Cu base composite properties are recommendable and this can be taken forward to different applications.

**Table 4.** Mechanical properties of Cu base composite with $Si_3N_4$ and AlN reinforcement.

| Sample no | Base metal | Hardness (HV) | Density (g/cc) | Porosity (%) |
|---|---|---|---|---|
| 1 | Cu | 49 | 6.1 | 2.4 |
| 2 | Cu – $Si_3N_4$NP | 59 | 6.24 | 1.9 |
| 3 | Cu – $Si_3N_4$μP | 68 | 6.19 | 2.7 |
| 4 | Cu – AlNNP | 54 | 5.70 | 2.6 |
| 5 | Cu – AlNμP | 65 | 5.57 | 3.1 |

## XRD Analysis

In the present work, the microstructural evaluation was supported by Scanning Electron Microscopy (SEM) and Energy-Dispersive Spectroscopy (EDS) analyses. The BSE images reveal that both nano- and micro-sized particles exhibit irregular morphologies with non-spherical geometry, which is typical of ceramic powders produced via solid-state synthesis (Fig. 6). The EDS spectra confirm the elemental composition of the reinforcements, with nano $Si_3N_4$ showing silicon and nitrogen concentrations of approximately 49.0% and 49.5% (Fig. 6a), respectively, and micro $Si_3N_4$ particles showing 49.7% Si and 48.9% N (Fig. 6c). Similarly, AlN particles in nano and micro forms exhibit aluminum contents of 55.78% and 56.3%, and nitrogen contents of 44.2% and 43.6%, respectively (Fig. 6b & 6d). These values indicate high purity (approximately 99%) and stoichiometric consistency across both size scales of reinforcements. The uniform elemental distribution in the EDS spectra suggests that no surface oxidation or contamination occurred during handling or processing. Moreover, the lack of foreign peaks or elemental deviations supports the chemical stability of the $Si_3N_4$ and AlN phases prior to their incorporation into the copper matrix. The SEM and EDS results indicate that the reinforcements maintained structural integrity during processing at 800 °C.

## Machinability of Cu base $Si_3N_4$ and AlN reinforced composite

The wire electrical discharge machining on the Cu base $Si_3N_4$/AlN reinforced composite material was estimated by varying the pulse on time (μs) for a constant voltage (50 V). In order to realize the machinability of the composite, the pulse off time has been kept within a boundary (10 & 30 μs) as they are not much influenced over the machinability of the material [24-

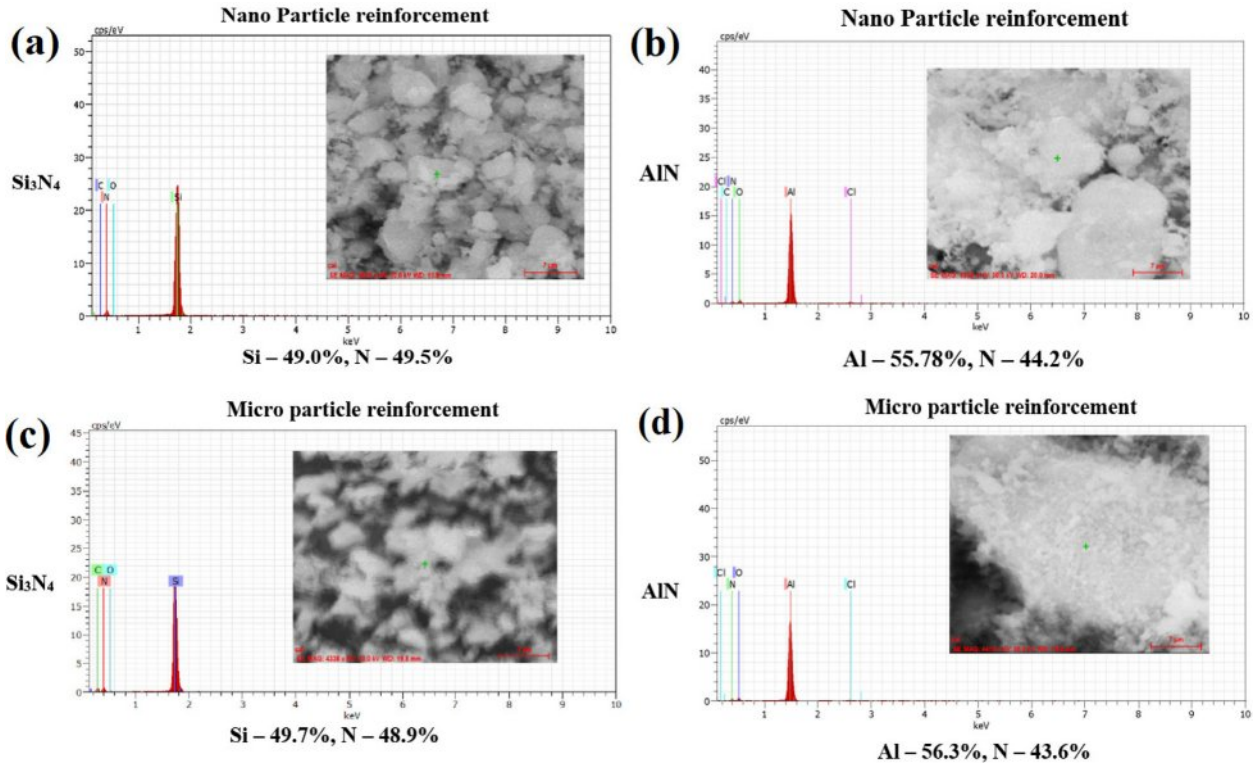


**Fig. 6.** BSE images and corresponding EDS spectra of reinforcement particles: (a) $Si_3N_4$ nanoparticles, (b) AlN nanoparticles, (c) $Si_3N_4$ microparticles, and (d) AlN microparticles, used in the copper matrix composite.

26]. Fig. 7 shows the surface roughness of Cu base $Si_3N_4$ reinforced composite at different pulse on time against the pulse off time – reinforcement particle. In general, the silicon nitride has high refractory index compared to the base metal. As the Cu base metal melts faster, surface roughness of the base metal (pure copper) sample reported with maximum surface roughness than the reinforcement. Electron image of the pure copper rod indicates the maximum recast layer after wire electrical discharge machining as depicted in Fig. 8. The surface is reflected with metal splats and oxide scales due to the partial melting of the layer. At a minimum pulse on time (110 µs), the surface roughness was found to be maximum (5.81 µm) at low level pulse of time (10 µs). And with respect to the increase in pulse on time, the surface roughness was found to be reduced to 4.07 µm. With the presence of $Si_3N_4$ in the Cu matrix material; the surface roughness was found to be reduced and controlled over the machined surface. The minimum surface roughness of 2.5 µm to a maximum of 4.27

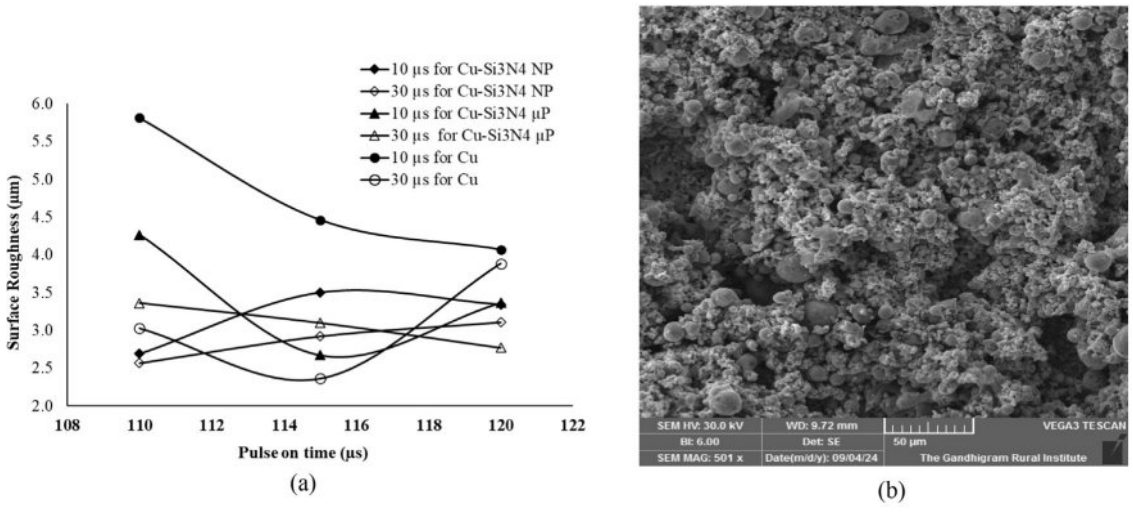


**Fig. 7.** (a) Surface roughness of the Cu base $Si_3N_4$ reinforced composite. (b) SEM image of pure Cu rod after machining.

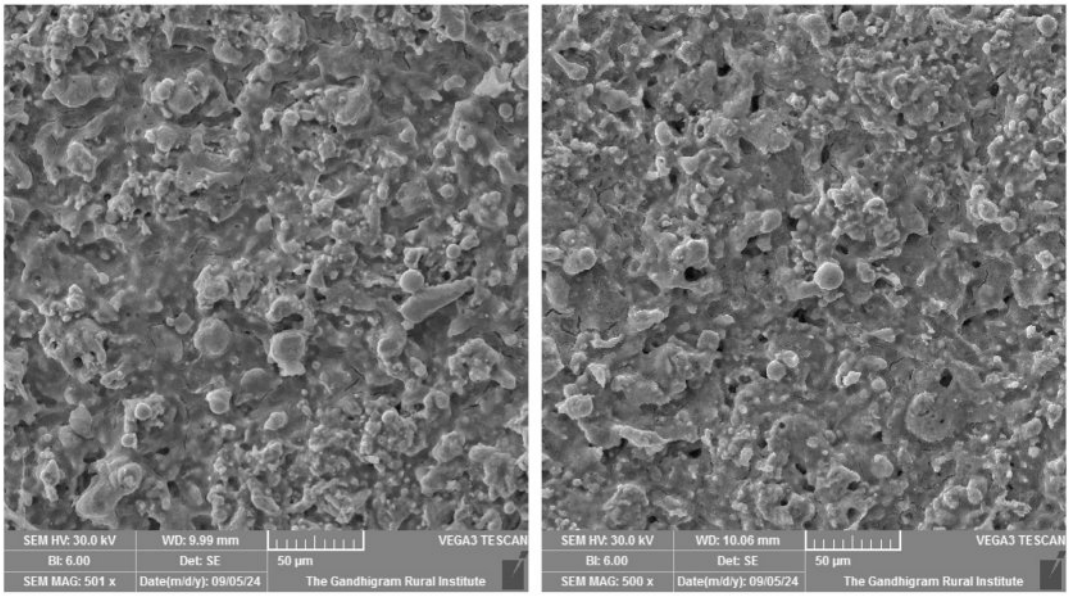


**Fig. 8.** SEM image of Si3N4 reinforced Cu composite rod after machining.

µm is measured for the $Si_3N_4$ reinforced Cu composite rod. Fig. 8 shows the similar surface morphology for both nano particle and micro particle reinforcement of $Si_3N_4$ in the Cu based composite rod. It is also noticed that, on the machined surface, the recast layer/partially melted zone has an impact of oxygen to form an oxide scale. About 15% to 17% in the $Si_3N_4$ reinforced Cu composite rod and maximum of 26% oxygen was noticed on the pure copper rod. From the experimental results it has been observed that, Cu was found to be a good conducting material.

In the same way, to the $Si_3N_4$ reinforcement, the surface roughness of AlN reinforced Cu composite rods is also measured and compared for this discussion (Fig. 9). Similar to the base matrix material, the conductivity of the AlN material was found to be more. The surface roughness values for the nano particle reinforcement (at a pulse duration of 110 µs – 30 µs) is 5.7 µm at an average which is found to be higher than 3.03 µm (for the same condition) of pure copper rod. The AlN micro particle reinforced Cu base composite has a maximum surface roughness value of 10.52 µm for a pulse span of 115 µs to 10 µs, with the surface roughness significantly increasing under all other conditions. Further machined surfaces are observed with electron microscopy and it has been noticed that, the AlN nano particle reinforced Cu rod has diffused splat and coarse ridges on the machined surface. On the other hand, the micro particle reinforced surface has agglomeration of oxide and reinforcements [27, 28]. The severity in the surface distraction was found to be catastrophic over the micro particle reinforced composite compared to

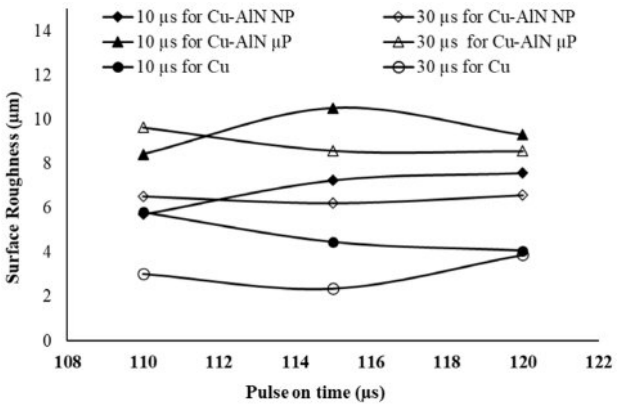


**Fig. 9.** Surface roughness of the Cu base AlN reinforced composite.

the nano particle reinforced composite (Fig. 10). Oxide formation rate in the micro reinforced Cu composite rod is maximum (11.47% from the spectra analysis) compared the nano particle reinforced composite (7%). Based on the inferences from the AlN reinforced composite, it is evident that nano particle with Cu matrix has superior bonding and machinability compared to the micro particle reinforcement [29, 30]. Also, it is found that the refractoriness of the $Si_3N_4$ in the Cu base composite is better than the AlN reinforced composite in terms of hardness, density and metallurgical quality. Further it is recommended to use $Si_3N_4$ in the Cu base composite for frictional components and mechanical loaded components.

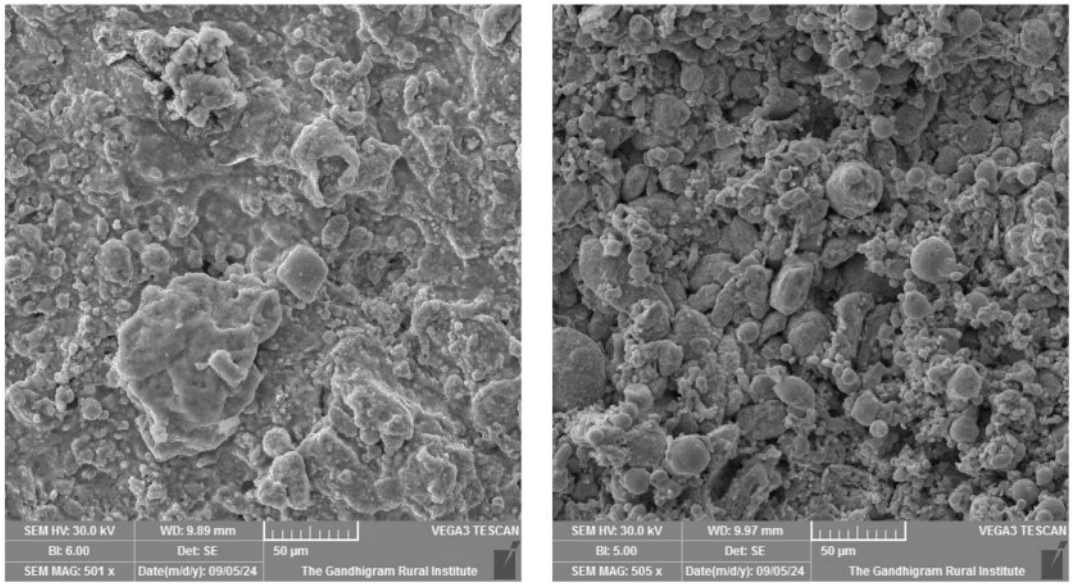


**Fig. 10.** SEM image of AlN reinforced Cu composite rod after machining.

## Conclusions

The present work successfully synthesized copper matrix composites reinforced with micro and nano particles of $Si_3N_4$ and AlN through powder compaction and sintering methods. Comprehensive characterization of the synthesied composites led to the following conclusions.

The $Si_3N_4$-reinforced composites with micro-sized particles, exhibited the highest microhardness (68 HV) and density (6.24 g/cc) levels, indicating improved reinforcement-matrix bonding and mechanical performance.

Furthermore, the AlN-reinforced composites showed better dispersion but lower density and hardness, reflecting their ductile nature and lower refractory properties compared to $Si_3N_4$.

Also, the porosity was found to be slightly higher in composites with micro-sized particles, owing to agglomeration and void formation during compaction.

The WEDM machinability tests revealed superior surface finish in $Si_3N_4$-based composites (the minimum surface roughness as low as 2.5 µm), while AlN-based samples, especially with micro particles, showed rougher surfaces and higher oxide formation due to poor thermal stability under discharge conditions.

Partially melted layer and oxide scales in the AlN reinforced Cu composite has increased the surface roughness to a drastic level compared to pure Cu and $Si_3N_4$ reinforced composite. The presence of aluminum in the matrix promoted surface oxidation, leading to ridge formation and a coarse-machined profile.

Overall, $Si_3N_4$ micro-reinforced copper composites demonstrated the better balance of mechanical strength and machinability, making them suitable for applications in frictional, tribological, and structural components where enhanced hardness and wear resistance are critical.

Based on the recommendations and results achieved, $Si_3N_4$ reinforced Cu composite outperforms better than AlN reinforced Cu composite. From the research findings it is evident that, $Si_3N_4$ reinforced Cu composite can be recommended for frictional components and mechanical force applied sections.

## References

1. C.A. León-Patino, G. Rodríguez-Ortiz, and E.A. Aguilar-Reyes, Mater. Des. 54 (2014) 845-853.
2. C. Real and F.J. Gotor, Heliyon 5[2] (2019) e01227.
3. M.R. Akbarpour and S. Alipour, Ceram. Int. 43[6] (2017) 13364-13370.
4. M.R. Akbarpour, H.M. Mirabad, F. Gazani, I. Khezri, A.A. Chadegani, A. Moeini, and H.S. Kim, J. Mater. Res. Technol. 27 (2023) 1317-1349.
5. Y.F. Yan, S.Q. Kou, H.Y. Yang, S.L. Shu, F. Qiu, Q.C. Jiang, and L.C. Zhang, Int. J. Extreme Manuf. 5[3] (2023) 032006.
6. D.-W. Shin and H. Guo, J. Ceram. Process. Res. 6[3] (2005) 263-265.
7. T. Jiang, H. Jin, Z. Jin, J. Yang, and G. Qiao, J. Ceram. Process. Res. 10[1] (2009) 113-116.
8. E. Şap, Ü.A. Usca, and M. Uzun, J. Braz. Soc. Mech. Sci. Eng. 44[9] (2022) 399.
9. E. Uhlmann, S. Piltz, and K. Schauer, J. Mater. Process. Technol. 167[2-3] (2005) 402-407.
10. F. Granados-Correa, J.L. Iturbe-García, and J. Bonifacio-Martínez, J. Ceram. Process. Res. 20[6] (2019) 597-602.
11. J.-M. Lee, B.-I. Kim, J.-H. Lee, K.-H. Kim, and M.-P. Chun, J. Ceram. Process. Res. 14[6] (2005) 707-711.

12. K.H. Hamzah, A.H. Abdulhussein, and M.N. Yasir, Metall. Mater. Eng. 30[2] (2024) 92-104.
13. M.A. Ahmed, W.M. Daoush, and A.E. El-Nikhaily, Adv. Mater. Res. 5[3] (2016) 131-140.
14. M. Kida, M. Bahraini, J.M. Molina, L. Weber, and A. Mortensen, Mater. Sci. Eng. A 495[1-2] (2008) 197-202.
15. M.S. Kang, K.H. Shin, D.W. Kim, S.J. Kim, T. Tran, and M.J. Kim, J. Ceram. Process. Res. 18[12] (2017) 848-853.
16. M. Zhang, L. Liu, S. Liang, and J. Li, Met. Mater. Int. 26[10] (2020) 1585-1595.
17. P. Kumaravel, K.V. Raja, and P. Suresh, J. Ceram. Process. Res. 24[3] (2023) 569-577.
18. T. Joyeux, J. Jarrige, J.C. Labbe, and J.P. Lecompte, Key Eng. Mater. 206 (2002) 555-558.
19. V. Muthusamy and T.R. Kumar, J. Ceram. Process. Res. 26[3] (2025) 418-431.
20. V.N. Gaitonde, S.R. Karnik, M. Faustino, and J.P. Davim, Int. J. Refract. Met. Hard Mater. 28[2] (2010) 221-227.
21. W. Węglewski, P. Pitchai, M. Chmielewski, P.J. Guruprasad, and M. Basista, Int. J. Heat Mass Transf. 188 (2022) 122633.
22. X. Cao, J. Duan, C. Wang, P. Jin, Y. Yang, and J. Zhang, Ceram. Int. 50[5] (2024) 7366-7373.
23. X. Li, Q. Zhang, W. Lou, F. Li, J. Liang, and S. Gu, Coatings 13[12] (2023) 2093.
24. X.M. Cao, J. Duan, C. Wang, P. Jin, Y. Yang, and J. Zhang, Mater. Today Commun. 38 (2024) 107722.
25. Y. Jiang, L. Xiao, P. Zhai, F. Li, Y. Li, Y. Zhang, Q. Zhong, Z. Cai, S. Liu, and X. Zhao, Surf. Coat. Technol. 456 (2023) 129264.
26. Y.J. Joo, J.W. Kim, K.B. Shim, and C.J. Kim, J. Ceram. Process. Res. 19[4] (2018) 342-346.
27. A. Kalemtas, G. Arslan, P. Kayab, S. Turan, and F. Kara, J. Ceram. Process. Res. 19[2] (2018) 119-125.
28. C.-H. Yang, C.-N. Yang, and Y.-C. Lee, J. Ceram. Process. Res. 18[9] (2017) 628-633.
29. F. Ali, B.S. Park, and J.S. Kwak, J. Ceram. Process. Res. 14[4] (2013) 529-534.
30. J.-M. Lee, B.-I. Kim, K.-H. Kim, and M.-P. Chun, J. Ceram. Process. Res. 14[6] (2013) 707-711.